CrystEngComm

Accepted Manuscript

ROYAL SOCIETY OF CHEMISTRY

www.rsc.org/crystengcomm

Journal Name

ARTICLE

Selective CO_2 Uptake and Vapor Adsorption Study within Sn(IV) Porphyrin Crystals

Received 00th January 20xx,
Accepted 00th January 20xx

DOI: 10.1039/x0xx00000x

www.rsc.org/

S. Wang,[a] G. P. Knowles,[a] A. L. Chaffee,[a] and S. J. Langford[a]

A systematic investigation of the effect that simple substituents attached to the phenolic ring have on the stability and adsorption properties of the porous crystals of parent Sn(IV) porphyrin diphenolates is made. A family of three dimensional honey-comb-like supramolecular porous materials (SPMs) was obtained by crystallisation of three different discrete porphyrin diphenolates Sn(IV)tTTP(*o*-cresol)$_2$ (**1**), Sn(IV)tTTP(*o*-bromo)$_2$ (**2**), Sn(IV)tTTP(*m*-nitro)$_2$ (**3**). Their structures and crystalline integrity were studied using single crystal X-ray diffraction and powder X-ray diffraction techniques, respectively. Vapor adsorption measurements on Sn(IV)tTTP(*o*-cresol)$_2$ revealed a guest uptake capacity. Gas adsorption investigations of these materials demonstrates that this class of SPMs retains high thermal stability and permanent porosity with functional groups lining the pores, which makes this Sn(IV) porphyrin diphenolates family a potential candidate for building high thermal stability SPMs.

Introduction

Seeking new materials with high stability and selective adsorption properties is of great significance for post-combustion capture.[1] Among the many absorbents, porous coordination polymers (PCPs) and metal-organic frameworks (MOFs) are well known for their high surface area, permanent porosity and selective adsorption properties.[2] Nevertheless, the development of these materials is some-what limited by the challenging synthesis of organic ligands and poor framework compatibility.[3] Indeed, it is still a challenge to functionalize and engineer porous frameworks with suitable pores and a tailor-made affinity while maintaining the structural topology needed to achieve highly selective separation and specific recognition.[4]

Compared to PCPs and MOFs, robust crystalline supramolecular porous materials (SPMs), including purely hydrogen bonding organic frameworks (HOFs) and non-hydrogen bonding supramolecular organic frameworks (SOFs), are not as well established due to the flexible nature of organic networks becoming unstable by not being able to maintain empty cavities after removal of the incorporated solvent, in many cases.[5, 31] Once an organic molecule is found as a suitable molecular scaffold or building block for SPMs, the opportunity to readily modify the components, but retain the macromolecular porous structure, would allow a wide range of functional diversifications both at the molecular level and at the supramolecular level.

Scheme **1**. Compounds used for constructing functionalized SPMs.

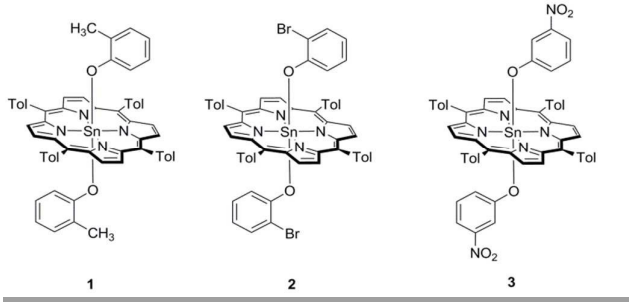

To obtain robust open pores based on a purely organic channel-type structure without the pores collapsing when included solvent is removed, is of general interest. Early in 2002, Langford et al. reported on the synthesis and crystal structures of two porous Sn(IV) porphyrin diphenolates[6] that both exhibited very good thermal stability as examined by the TGA analysis. More of these Sn(IV) porphyrin diphenolates SMPs were constructed by our group in recent years.[7] These robust frameworks not only possess a good tolerance to large and dissymmetric phenolates, but demonstrated that channel surface functionalisation can be realized via substitution on the axial phenolic rings. With the right development, such organic molecular porous materials may find useful applications in gas storage and separation.

Here, the structure and adsorption properties of Sn(IV)tTTP(*o*-cresol)$_2$ (**1**)[7], against two new Sn(IV) porphyrin diphenolates Sn(IV)tTTP(*o*-bromo)$_2$ (**2**), Sn(IV)tTTP(*m*-nitro)$_2$ (**3**) are examined. These compounds showed considerable promise as building blocks with which to form novel porous materials.

[a] School of Chemistry, Monash University, Victoria, Australia 3800.

Electronic Supplementary Information (ESI) available: [X-ray crystallographic file (CIF) of compound **2**-**3** and cyclohexane included **1**. PXRD spectra of acid or base immersed compound **1**. TGA spectra of n-hexane vapour uptake in 1 at 40 and 60 °C. 400 MHz ^{1}H NMR spectra of different solvent-loaded compound **1**. See DOI: 10.1039/x0xx00000x

Compound **2** was rationally designed to substitute the methyl group in **1** with the bromo group within the pore lining. This should also have an effect of increasing the surface area and total accessible volume due to its comparable smaller molecular volume. Compound **3** was designed to introduce the nitro group onto the channel surface to facilitate local dipole/quadrupole interactions through the nitro oxygen atoms thereby hopefully facilitating stronger CO_2 interactions, which would be absent for the fully aliphatic functionalized surface in **1** (Scheme 1).

Experimental

Chemicals and suppliers

Pyrrole ACS grade 98%, p-Tolualdehyde FG. 97%, Tin(II) chloride dihydrate ACS reagent 98%, o-cresol Kosher 99%, m-nitrophenol reagent plus 99%, o-bromophenol 98%, sodium 99.9% trace metals basis, calcium hydride reagent grade 95%, pyridine reagent grade 98% (Sigma-Aldrich), propionic acid GC, potassium carbonate-1.5-hydrate (Merck), Tetrahydrofuran ACS reagent grade (Merck) was stored over sodium wire and redistilled prior to use, dichloromethane GC (Merck), chloroform GC (Merck) was distilled from calcium hydride, cyclohexane anhydrous 95%, n-hexane anhydrous 95%, benzene anhydrous 99.8%, toluene anhydrous, p-xylene anhydrous 99% (Sigma-Aldrich), All gases used (Ar, N_2, CO_2, H_2, CH_4) are of high purity (BOC). Distilled water was used for all aqueous manipulations.

PXRD analysis

Approximately 30 mg of the Sn(IV) porphyrin diphenolates were soaked in water, dispersed and dried as a thin layer on a stainless plate before the PXRD measurements. PXRD data were collected at ambient temperature in an air atmosphere on a Philips 1130 powder x-ray diffractometer with monochromatic Cu Kα1 radiation (λ = 1.540 Å) operated in Bragg-Brentano geometry.

Thermal analysis

Thermal gravimetric analyses were performed on a Mettler Toledo instrument heated from 50 to 500 °C with a scan rate of 2°C min-1 with in flowing nitrogen.

NMR analysis

^{1}H nuclear magnetic resonance (NMR) spectra were recorded using a Bruker DRX 400 MHz spectrometer (400 MHz for ^{1}H NMR), using deuterated chloroform ($CDCl_3$) unless otherwise stated. Chemical shifts are reported relative to the resonances of residual $CHCl_3$ at δ = 7.26 (H). Each resonance was assigned according to the following convention: chemical shift (δ) measured in parts per million (ppm), multiplicity, coupling constant (*J* Hz), number of protons and assignment. Multiplicities are denoted as (s) singlet, (d) doublet, or (m) multiplet.

Single Crystal X-ray Diffraction (SCXRD)

X-ray crystal diffraction patterns are determined using an Enraf Nonius FR 590 Kappa CCD diffractometer or a Brüker Kappa Apex II diffractometer with graphite-monochromated Mo Kα radiation (λ = 0.71 Å) at 123K unless otherwise stated. Indexing was performed using APEX2.[8] Data integration and reduction were completed using SaintPlus 6.01.[9] Absorption correction was performed by the multi-scan method implemented in SADABS.[10] The space group was determined using XPREP implemented in APEX2.1 The structure was solved with SHELXS-97[11] (direct methods) with the graphical interface X-Seed v2.0,[12] and refined on F2 (nonlinear least-squares method) with SHELXL-97 contained in APEX2, WinGX v1.70.01,[13] and OLEX2 v1.1.5[14] program packages. All non-hydrogen atoms were refined anisotropically. Crystallographic data in CIF format have been deposited at the Cambridge Crystallographic Data Center as supplementary publication no. 1435075-1435078. The contribution to SCXRD data by uncoordinated guests was estimated using PLATON/ SQUEEZE,[15] as executed on the framework model with the largest of any coordinated molecules remaining.

Gas Adsorption Analysis

N_2, CO_2, CH_4, and H_2 adsorption measurements were obtained via a Micromeritics Tristar II 3020 gas sorption analyser using high purity gases. Helium was used to calculate free space measurements. Analytes were initially pre-degassed under dynamic vacuum at 250 °C overnight via a Micromeritics VacPrep 061 degasser, backfilled with N_2, and then accurately weighed within 0.1 mg prior to transfer for analysis. BET surface area (SA) was calculated from adsorption data collected over the partial pressure range 0.05-0.30. Total pore volumes (PV) were estimated from the amount of N_2 adsorbed at relative pressure 0.997 (pores < 660 nm diameter). The pore size distribution (PSD) is calculated from the N_2 adsorption isotherm, $N_{exp}(p/p_0)$, at 77 K by solving the integral adsorption equation.[16] Micropore analysis method (MP method) was employing Harkins and Jura thickness equation at relative pressure of 0.34.[17]

Vapour Adsorption Analysis

Vapour adsorption was measured with a Setaram TAG 24 simultaneous symmetrical thermogravimetric analyser. Materials as synthesised were initially loaded onto the analyser and dried to constant mass under 70 ml min^{-1} N_2 at 260 ◦C for around 6 hours. The same materials were used directly for the next round of measurement, which were again re-activated, post adsorption analysis then re-weighed to examine re-generation of the sorbent. The gas flow control system was set up according to literature,[18] except that 35 ml min^{-1} of N_2 was continuously supplied to the balance housing from one mass flow controller, and the other 33 ml min^{-1} of N_2 was supplied evenly to both the reference and sample furnaces after passing through glass sinters submerged in 200 mL cyclohexane or *n*-hexane (10 ◦C) respectively, from separate mass flow controllers.

Chemical Stability

The chemical stability of compound **1** toward acid and base was studied by trading the as-synthesized materials (100 mg) with solutions (10 mL) of 6.0 M HCl and 6.0 M NaOH, respectively, for 7 days at room temperature. After the treatment, the solids were filtered and dried before the PXRD analysis (Figure S1 Supporting Information) was performed. All samples showed an unaltered diffraction pattern.

Preparation of bisphenolates 1-3

Thermal gravimetric Sn(IV)tTTP$(OH)_2$ was synthesized based on the method reported by Arnold.[19] Synthesis of compound **1**-**3** was achieved by using well-established procedures.[20] Sn(IV)tTTP$(OH)_2$ (82.2 mg, 0.1 mmol) was added to 2 equivalents of *o*-cresol (21.6 mg, 0.2 mmol) in base-washed $CHCl_3$ and the solution was left to stir at room temperature for 2 days, monitored for completion by taking aliquots for NMR analysis. Sn(IV)tTTP(*o*-bromo)$_2$ (**2**), and Sn(IV)tTTP(*m*-nitro)$_2$ (**3**) were synthesized analogously by replacing 2-methylphenol with the equivalent molar amounts of 2-bromophenol and 3-nitrophenol, respectively. Purple needle-shaped crystals of the Sn(IV) complexes were collected by slow diffusion of *n*-hexane into a concentrated dichloromethane solution of **1-3**. Their purity was examined by ^{1}H NMR spectroscopy using the anisotropy of the porphyrin to distinguish between bound and free phenol. Sn(IV)tTTP(*o*-bromo)$_2$ (2) ^{1}H NMR (400 MHz, $CDCl_3$, 300 K) δ = -1.29 (s, 6 H, phenol-methyl group), 1.06 (d, *J* = 1.2 Hz, 1 H, ArH), 1.08 (d, *J* = 1.6 Hz, 1 H, ArH), 2.74 (s, 12 H, *meso*-ArCH_3), 5.41 (m, *J* = 6.4 Hz, 2 H, ArH), 5.54 (m, *J* = 6.4 Hz, 2 H, ArH), 5.59 (m, *J* = 6.0 Hz, 2 H, ArH), 7.59 (d, *J* = 8.0 Hz, 8 H, *meso*-ArH), 8.04 (d, *J* = 8.0 Hz, 8 H, *meso*-ArH), 9.09 (s, 8 H, *β*-pyrrolic H). Sn(IV)tTTP(*m*-nitro)$_2$ (3) ^{1}H NMR (400 MHz, $CDCl_3$, 300 K) δ = -1.29 (s, 6 H, phenol-methyl group), 1.06 (d, *J* = 1.2 Hz, 1 H, ArH), 1.08 (d, *J* = 1.6 Hz, 1 H, ArH), 2.74 (s, 12 H, *meso*-ArCH_3), 5.41 (m, *J* = 6.4 Hz, 2 H, ArH), 5.54 (m, *J* = 6.4 Hz, 2 H, ArH), 5.59 (m, *J* = 6.0 Hz, 2 H, ArH), 7.59 (d, *J* = 8.0 Hz, 8 H, *meso*-ArH), 8.04 (d, *J* = 8.0 Hz, 8 H, *meso*-ArH), 9.09 (s, 8 H, *β*-pyrrolic H).

Results and discussion

Single crystal X-ray diffraction studies of the new compounds **2** and **3** revealed they are conformational analogues of compound **1**. Both compounds **2** and **3** crystalize in the *R*-3 space group, and the Sn(IV) centre adopts the same octahedral geometry as which had been observed in compound **1**. The effective packing of the rigid macrocycles through C-H···O hydrogen bonding and van der Waals interactions provide a three dimensional honeycomb-like structure with hour-glass shaped 1D channels running along the supramolecular structures with a diameter of 9.0 Å, 10.0 Å, 10.0 Å for compounds **1**, **2** and **3** respectively. Interestingly, the introduction of the *ortho*-substituted halogen group, or the meta-nitro group didn't change the macromolecular pore configuration appreciably. Clearly shown (Figure 1) is that the new functionality appears to line the honey-comb like three dimensional structure thereby potentially changing the nature

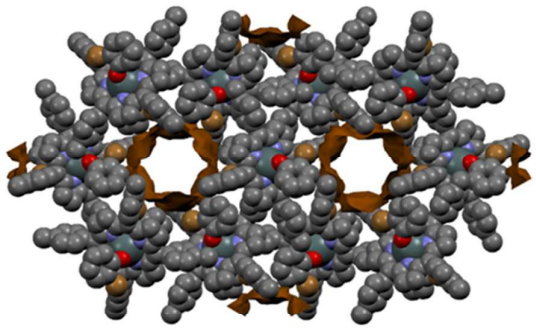

Sn(IV)tTTP(*o*-bromo)$_2$ 2

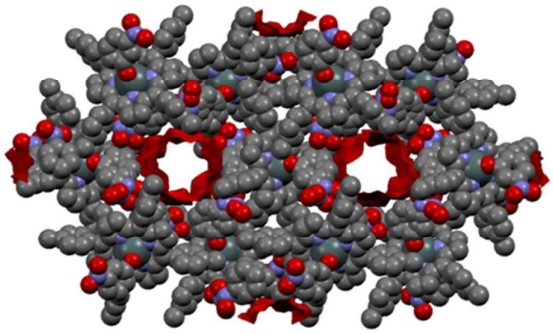

Sn(IV)tTTP(*m*-nitro)$_2$ 3

Figure 1. Space-filling mode of compounds **2** and **3** down the crystallographic *c* axis featuring one-dimensional channels

of the adsorption properties. If generalised, the possibility to construct more porous porphyrin structures with a range of diversity and variability could be important to identifying novel designer adsorbents. In contrast, some other porous porphyrin-bearing structures have been documented in the past as part of larger metal-organic frameworks, there appear to be intolerant to functionalisation as the pyridyl group on porphyrin motif played a crucial role for the construction of the porous structures.[21]

Further detailed inspection into the structure of **2** revealed close contacts supporting weaker interactions including C-Br···H (distance = 3.01 Å) and C-H···π interactions (distance = 2.77-2.89 Å) occur between two adjacent building blocks, which may further stabilize the whole supramolecular network.

The total solvent accessible volume of evacuated compound **1**-**3** revealed a large calculated occupiable and accessible void volume of 9.5 % (1145 Å^3 per unit cell), 13.2 % (1602 Å^3 per unit cell) and 13.4 % (1624 Å^3 per unit cell) for a 1.4 Å probe radius (that is, the van der Waals radii for a water molecule), respectively.[22] The integrity and robustness of compounds **1**-**3** were confirmed by powder X-ray diffraction studies on the solvate filled (blue line) and evacuated (wine line) network solids (Figure 2). All of the peaks in red and/or blue in the PXRD pattern can be indexed well according to the simulated pattern (black) from the crystal structure of self-assembled

(a)

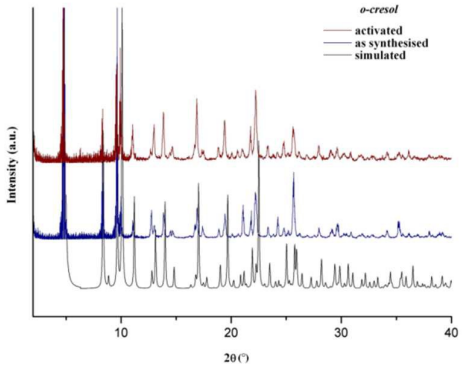

(b)

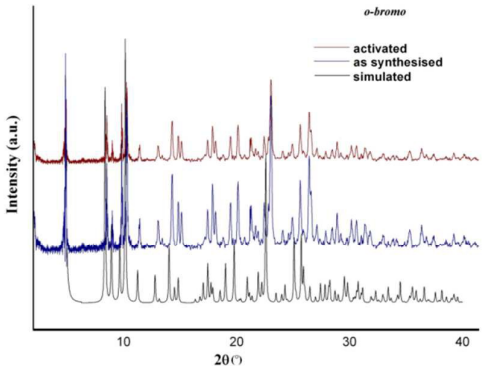

(c)

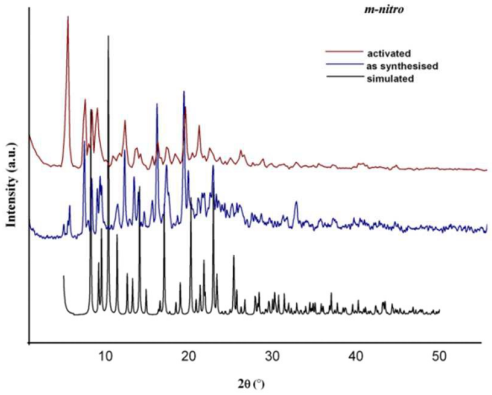

Figure 2. PXRD spectra of SPMs (a) **1**; (b) **2**; (c) **3**. Simulated (black), as synthesized (blue) and desolvated (red).

compounds **1**-**3**. In contrast to the structure generated by **3**, no solvent was observed in the channels of **2** by sc-XRD, and confirmed by the PLATON/SQUEEZE programme, showing no real electron density exists in the cavities of the single crystal structure (see SI).

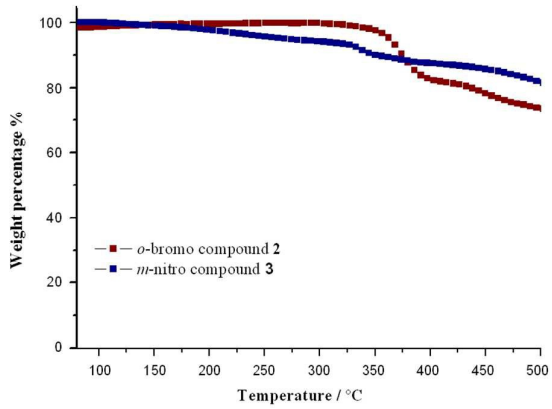

Figure 3. TGA curves of SPMs **2** (red), and **3** (blue).

Thermal stability

Thermal gravimetric analysis (TGA) was carried out to examine the thermo stability of as prepared compounds **2** and **3**. Previous thermal gravimetric analysis (TGA) on **1** showed a small percentage weight loss from 80 °C to 190°C, attributable to loosely held solvate molecules, with no obvious weight loss observed from 190 to 350 °C, after which the desolvated framework began to decompose.[7] Unlike **1**, the TGA of **2** revealed excellent thermal stability up to 350 °C before decomposition (Fig. 3). The level of thermal stability of this framework as evidenced by the trace in Figure 2 supports the inference that no solvent was included in the single crystal structure during crystallisation indicating its potential ability to capture and release small molecules with suitable size and physiochemical properties. Thermogravimetric analysis of **3** is more typical of what was expected. Temperatures >150°C lead to a consistent loss of weigh to 250°C consistent with the loss of entrapped solvent molecules. As opposed to **2**, no marked decomposition point was visible indicating a difference in the behaviour of the frameworks.

Gas adsorption studies

The N_2 adsorption isotherms collected at 77 K for the activated SPMs **1**-**3** showed a typical Type-I isotherm characteristic of a microporous material (Figure 4). The estimated Brunauer–Emmett–Teller (BET) surface areas of **1-3** were calculated as 173, 229 and 146 m^2g^{-1}, respectively. While the N_2 desorption isotherm for **3** indicated a reversible sorption process, a pronounced hysteresis was observed, attributed to the capillary condensing effect.[23] The total pore volume estimated from the N_2 adsorption isotherms for compounds **1**-**3** were calculated using non-local density functional theory modelling. Values of 0.131 $cm^{-3}\cdot g^{-1}$, 0.137 $cm^3\cdot g^{-1}$ and 0.106 $cm^3\cdot g^{-1}$ respectively for **1-3**, are comparable to some of the best performing single component SPMs.[24] The pore size distribution for **1**-**3** was calculated using the same model for N_2 adsorption isotherm and the MP-method for the CO_2 adsorption isotherm were found to be in good agreement (Figure 4 inset), and consistent with the channel diameters

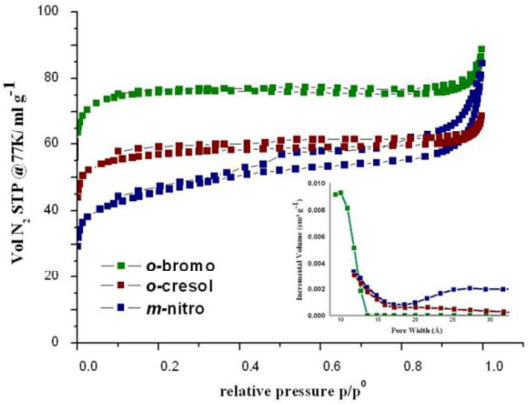

Figure 4. N_2 adsorption/desorption isotherms for SPMs **1**-**3** at 77K. Inset: pore size distribution of **1**-**3** calculated from NLDFT models.

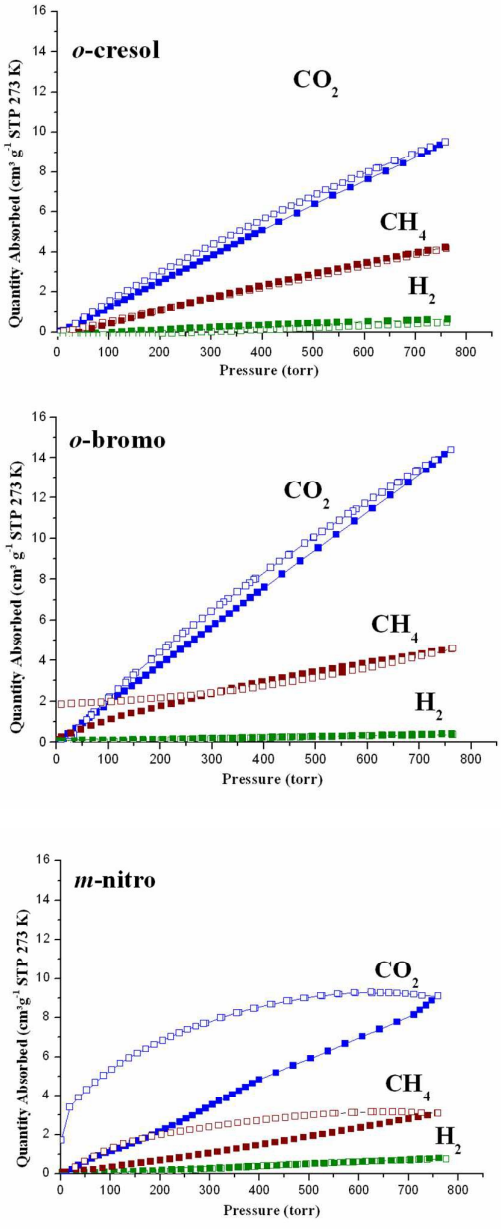

Figure 5. CO_2, CH_4, H_2 adsorption/desorption isotherms for SPMs **1**-**3** at 273K.

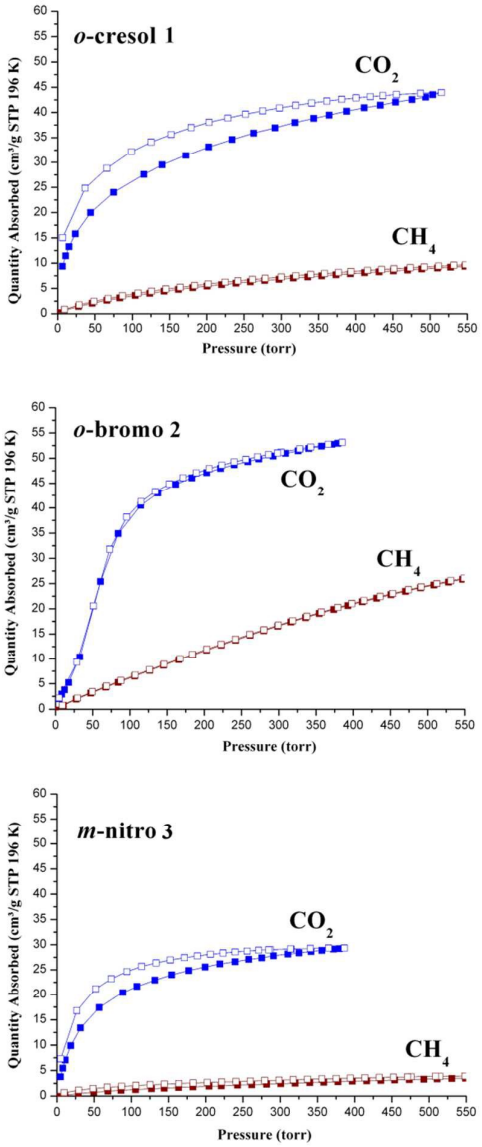

Figure 6. CO_2, CH_4 adsorption/desorption isotherms for compound **1**-**3** at 196 K.

Calculated from their single crystal X-ray structures. Even though the BET surface area of activated **1**-**3** is somewhat smaller than those of MOFs containing similar 1-D channels, their pore volumes are comparable.[25]

The selectivity of **1**-**3** with regard to CO_2, CH_4 and H_2 gases were measured volumetrically up to 1 bar at 273 K under isothermal conditions (Figure 5). Surprisingly, SPMs **1**-**3** displayed very weak absorption for H_2 gas, up to ~0.5 cm^3 g^{-1} under the conditions used, which may attributed to the low

interaction energy[26] (normally less than 10 kJ mol^{-1}) between physisorbed hydrogen molecules and the porous surface. It was anticipated a stronger sorption of hydrogen to the pi surface of the porphyrin components. The adsorption of CH_4 gas for SPM **1**-**3** was also quite low when compared to other reported supramolecular porous materials (SPMs),[27] but each SPM revealed slight differences, which may be ascribed to the features of materials such as surface area, free volume framework density and functionalization of the pore. Despite no appreciable uptake of CO_2 (kinetic diameter: 4.0 Å) with reversible uptakes of 10 $cm^3 g^{-1}$ (0.4 mmol g^{-1}) for **1**, 16 $cm^3 g^{-1}$ (0.7 mmol g^{-1}) for **2** and 9 cm^3 g^{-1} (0.4 mmol g^{-1}) for **3**, the single component pure gas isotherms suggested compounds **1**-**3** would show a moderate selectivity as high as 6:1 for CO_2 over CH_4. We surmise the relative low uptake of CO_2 for SPM **1**-**3** could be caused by the highly non-polar environment provided by the tolyl groups. Interestingly, the CO_2 desorption for SPM **3** exhibited a degree of hysteresis at 273 K, indicating its greater affinity for CO_2 once absorbed.

The CO_2 and CH_4 adsorption isotherms for SPMs **1**-**3** at 195K are compared in Figure 6. The CO_2 uptake for SPM **2** (54 $cm^3 g^{-1}$) is the highest within the series, and at 373 torr (SPM **1** = 36 $cm^3 g^{-1}$, and SPM **3** = 27 $cm^3 g^{-1}$) is comparable with reported SOFs at the same pressure.[5] The S-shape character of the isotherm in the low-pressure region (0-75 torr) for **2** has been observed previously for inflexible frameworks and can be attributed to attractive electrostatic interactions between CO_2 molecules.[28]

The CH_4 adsorption data for SPMs **1**-**3** indicate fully reversible uptake of 9 $cm^3 g^{-1}$, 27 $cm^3 g^{-1}$ and 5 $cm^3 g^{-1}$ at 550 torr, respectively. Although SPM **2** shows the best CO_2 uptake, the selectivity CO_2/CH_4 for **2** (2.5 : 1) is not as high at 373 torr. Owing to a reduction in the CH_4 uptake across the three examples, the CO_2/CH_4 ratio improves for **1** (5 : 1) and **3** (11 : 1) at the same pressure. The nitro functionality appears to endow the SPM with a higher CO_2/CH_4 selectivity over the entire pressure range measured. This behaviour can be explained by the higher charge density sites of the portal which might facilitate local-dipole/quadrupole interactions with CO_2 that would be absent for CH_4 and H_2. The absorbed CO_2 in SPMs **1**-**3** can be mostly regenerated by the pressure swing process and any trace CO_2 remaining can be fully liberated by heating at 200 ° C under vacuum.

Vapour adsorption studies of SPM 1

The microporous nature of our Sn(IV) porphyrin diphenolate SPMs combined with the hydrophobic nature of SPM **1** encouraged us to explore its potential for vapour uptake. The solvent vapour sorption of single crystals of SPM **1** were measured using TGA, with a 5% *v/v* solvent vapour in N_2 gas at 40 °C and 60 °C for cyclohexane and n-hexane. The uptake for other non-polar solvent vapours such as benzene, toluene and para-xylene were examined differently by exposure activated exchange under an atmosphere of the corresponding solvent vapour at 40 °C overnight, and confirmed by ^{1}H NMR analysis after drying the solvent-loaded sample at 80 °C in air.‡

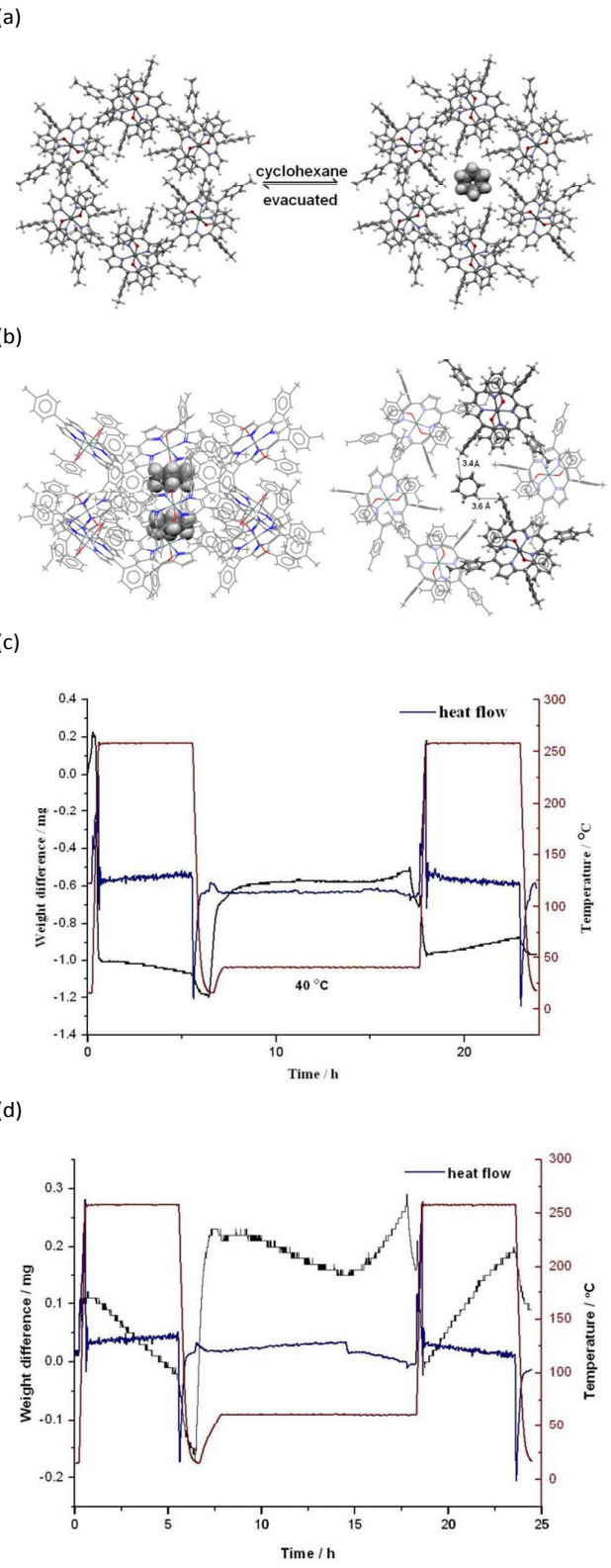

Figure 7. Cyclohexane vapour uptake in SPM **1** with (a) single-crystal-to-single-crystal transformation, (b) schematic view along *b* axis of 1 ⊂ cyclohexane single crystal structure, (c) weight change upon cyclohexane vapour uptake at 40 °C, (d)

weight change upon cyclohexane vapour uptake at 60 °C. Temperature change upon time (wine), weight change upon time (black), heat flow change upon time (blue).

Cyclohexane vapour uptake at 40 °C and 60 °C are compared in Figure 7. A 1.96 wt % change was observed at 40 °C for **1** (Figure 7c), corresponding to ~0.25 cyclohexane molecules per formula unit of the desolvated samples, which is in good agreement with the single-crystal-to-single-crystal (SCSC) transformation in loading cyclohexane into the sample (~0.23 cyclohexane molecule per formula unit, Figure 7a). During the transformation of desolvated 1 into 1 ⊂ cyclohexane, no substantial change was observed in the unit-cell parameters and the window size of the 1D channels in comparison to the parent host lattice (see SI). Further inspection of the inclusion complex suggested that the cyclohexane molecules align in parallel with each other in the centre of channel with a snug fit leading to close contacts between the cyclohexane and tolyl groups (C-H···C 3.4-3.6 Å, Figure 7b).

Cyclohexane vapour uptake at 60 °C revealed similar trend at first as that at 40 °C, but the sorption curve showed a big fluctuation as the measuring time increased, which can be explained by a dynamic equilibrium process at 60 °C (Figure 7d). While accurate determination of the location and packing of non-coordinating cyclohexane was successful, the crystallographic modelling of other guests proved to be more challenging. We attribute this both to the dynamic nature of these guests, leading to large atomic displacement parameters, and to the fact that their molecular symmetries were in most cases lower than the crystallographic site symmetries,[29] leading to partial atom site occupancies.

Vapour adsorption of n-hexane into SPM **1** at both 40 and 60 °C showed much slower adsorption rate compare with that of cyclohexane at similar temperatures (Fig. S2, SI). The adsorption difference may demonstrate the combined influence of size effect and adsorbent-adsorbate interaction. The amount of absorbed benzene, toluene and para-xylene were calculated by ^{1}H NMR analysis, which suggests the ratio of guest to Sn (IV) porphyrin diphenolates is 1 : 1. (SI). As a result, the influence of different thermodynamic effects and inter-pore steric hindrance (size exclusion) on total guest uptake for different solvent vapour was not obvious as small hydrophobic guests can be favourably absorbed into the 9 Å diameter channel.

Conclusions

In summary, this work reports on the generation of a functional supramolecular networks – the so-called SPMs - incorporating Sn(IV) porphyrin phenolates. The supramolecular arrangements were engineered through appropriate functionalisation of the phenolic rings of discrete Sn (IV) porphyrin diphenolates. All SPMs are crystalline, robust and show permanent porosity as confirmed by PXRD and reversible gas and vapour sorption investigations. Although the total gas uptake amount is disappointing in terms of generating a potential CO_2 storage material based on organic crystals, it does nevertheless demonstrate the principle and encourages future studies in this area. The crystals of **1** showed certain resistance to acid/base aqueous solution, and such high acid/base stability has rarely been documented in SPMs and is also not common in reported MOFs.[30] Obviously, the close packing and cooperative supramolecular interactions combining with its hydrophobic pore surface nature is crucial for the improved stability. The synthesis and design strategy described herein demonstrates the feasibility to rational design to construct robust supramolecular porous porphyrin diphenolate networks. Future exploration in construction of sorbent materials towards improvement of the separation performance for CO_2/CH_4 mixtures is underway. Moreover, although there are several examples of exchanging solvent guests in similar porphyrin MOFs structures, this is the first observation of incorporating solvent molecules into open porphyrin channels with SCSC transformations in discrete supramolecular porphyrin materials, which implies further investigation of porous solids based on supramolecular assembled porphyrin molecules for solvent purification is warranted.

Acknowledgements

Financial support from Monash University is gratefully acknowledged. Ms Wang would like to thank the Australian Government for the allocation of an Australian Postgraduate Award.

Notes and references

‡ The TGA approach was not used for these solvents due to incompatible solvents for instrumental requirement.

1 M. Wang, A. Lawal, and P. Stephenson, *Chemical Engineering Research and Design*, 2011, **89**, 1609; K. Sumida, D. L. Rogow, and J. A. Mason, *Chemical Reviews (Washington, DC, United States)*, 2012, **112**, 724; Y. Lv, G. Yan, and C. Xu, *Advanced Materials Research (Durnten-Zurich, Switzerland)*, 2013, **602-604**, 1140; M. Lucquiaud, E. S. Fernandez, and H. Chalmers, *Energy Procedia*, 2014, **63**, 7494; Q.-z. Li, M.-q. Chen, and F.-d. Meng, *Xiandai Huagong*, 2012, **32**, 82; Z. H. Lee, K. T. Lee, and S. Bhatia, *Renewable & Sustainable Energy Reviews*, 2012, **16**, 2599; S. D. Kenarsari, D. Yang, and G. Jiang, *RSC Advances*, 2013, **3**, 22739; N. Hedin, L. Andersson, and L. Bergstroem, *Applied Energy*, 2013, **104**, 418; H. Fahlenkamp and M. Dittmar, *Efficient Carbon Capture for Coal Power Plants*, 2011, 201; A. Chikukwa, N. Enaasen, and H. M. Kvamsdal, *Energy Procedia*, 2012, **23**, 82; A. S. Bhown, *Energy Procedia*, 2014, **63**, 542.

2 Z. Hasan and S. H. Jhung, *Journal of Hazardous Materials*, 2015, **283**, 329; X.-y. Yang, H.-l. Fan, and X.-l. Wang, *Tianranqi Huagong*, 2013, **38**, 85; M. Nomura, *Maku*, 2013, **38**, 31; R. Matsuda, *Adsorption News*, 2013, **27**, 3; J. Tian, P. K. Thallapally and B. P. McGrail, *Supramolecular Chemistry: From Molecules to Nanomaterials*, 2012, **6**, 3133; J. Liu, K. Thallapally Praveen, B. P. McGrail, R. Brown Daryl and J. Liu, *Chemical Society reviews*, 2012, **41**, 2308; Z. Zhang, S. Xiang and B. Chen, *Crystal Engineering Communications*, 2011, **13**, 5983, J.-R. Li, R. J. Kuppler and H.-C. Zhou, *Chemical Society Reviews*, 2009, **38**, 1477-1504.

3 L. D. Belyakova, A. V. Kiselev, and N. P. Platonova, *Advances in Colloid and Interface Science*, 1984, **21**, 55; I. J. Jakovac, *Catal. Supports Supported Catal.*, 1987, 187, M. Eddaoudi, D. B. Moler, and H. Li, *Accounts of Chemical Research*, 2001, **34**, 319; G. Ferey, *Nature Materials*, 2003, **2**, 136; W. Lin, *Journal of Solid State Chemistry*, 2005, **178**, 2486; M. Vallet-Regi, F. Balas and D. Arcos, *Angewandte Chemie, International Edition*, 2007, **46**, 7548; R. L. Albright, *Official Proceedings - International Water Conference*, 2008, **69th**, ALBR/1-ALBR/22; F. Song, T. Zhang, and C. Wang, *Proceedings of the Royal Society A: Mathematical, Physical and Engineering Sciences*, 2012, **468**, 2035; C. M. Doherty, D. Buso, and A. J. Hill, *Accounts of Chemical Research*, 2014, **47**, 396; S. Qiu, M. Xue and G. Zhu, *Chemical Society Reviews*, 2014, **43**, 6116; S. Yaqub, N. Mellon and A. M. Shariff, *Applied Mechanics and Materials*, 2014, **625**, 237; H. Furukawa, U. Mueller and O. M. Yaghi, *Angewandte Chemie, International Edition*, 2015, **54**, 3417; T. M. Nenoff, *Nature Chemistry*, 2015, Ahead of Print; M. C. So, G. P. Wiederrecht, and J. E. Mondloch, *Chemical Communications (Cambridge, United Kingdom)*, 2015, **51**, 3501.

4 Y. He, Z. Zhang, S. Xiang, and F. R. Fronczek, *Chemistry - A European Journal*, 2012, **18**, 613; P. Falcaro, A. J. Hill, and K. M. Nairn, *Nature Communications*, 2011, **2**, 1234.

5 A. I. Cooper, *Angewandte Chemie - International Edition*, 2012, **51**, 7892; J. Tian, P. K. Thallapally and B. P. McGrail, *Crystal Engineering Communications*, 2012, **14**, 1909; N. B. McKeown, *J. Mater. Chem.*, 2010, **20**, 10588; P. S. Nugent, V. L. Rhodus and T. Pham, *J. Am. Chem. Soc.*, 2013, **135**, 10950; X. Z. Luo, X. J. Jia and J. H. Deng, *J. Am. Chem. Soc.*, 2013, **135**, 11684; W. Yang, B. Li, and H. Wang, *Crystal Growth and Design*, 2015, **15**, 2000; P. Li, Y. He, and J. Guang, *Journal of the American Chemical Society*, 2014, **136**, 547; P. Li, Y. He, and H. D. Arman, *Chemical communications*, 2014, **50**, 13081; P. Li, Y. He, and Y. Zhao, *Angewandte Chemie - International Edition*, 2015, **54**, 574; Y. He, S. Xiang and B. Chen, *Journal of the American Chemical Society*, 2011, **133**, 14570; T.-H. Chen, I. Popov, and W. Kaveevivitchai, *Nature Communications*, 2014, **5**, 5131; X. Z. Luo, X. J. Jia, and J. H. Deng, *Journal of the American Chemical Society*, 2013, **135**, 11684; M. Mastalerz and I. M. Oppel, *Angewandte Chemie - International Edition*, 2012, **51**, 5252; J. Lü, C. Perez-Krap, and M. Suyetin, *Journal of the American Chemical Society*, 2014, **136**, 12828; W. Yang, A. Greenaway, and X. Lin, *Journal of the American Chemical Society*, 2010, **132**, 14457.

6 G. D. Fallon, M. A.-P. Lee and S. J. Langford, *Organic letters*, 2002, **4**, 1895.

7 S. Wang, C. Forsyth and S. J. Langford, *Crystal Engineering Communications*, 2015, **17**, 3060; S. J. Langford and C. P. Woodward, *Crystal Engineering Communications*, 2007, **9**, 218.

8 Bruker, *(APEX2)*, (2010) Bruker AXS Inc., Madison,Wisconsin, USA.

9 Bruker, *SAINT. Data Reduction Software*, (2009) Bruker AXS Inc., Madison, Wisconsin, USA.

10 G. M. Sheldrick, *SADABS*, (2008), University of Gottingen, Germany.

11 G. M. Sheldrick, 1997; G. M. Sheldrick, *Acta Cryst.*, 1990, **A46**, 467; G. M. Sheldrick, *Acta Cryst.*, 2008, **A64**, 112.

12 L. J. Barbour, *Journal of Supramolecular Chemistry*, 2001, **1**, 189.

13 L. J. Farrugia, *Journal of Applied Crystallography*, 1999, **32**, 837.

14 O. V. Dolomanov, L. J. Bourhis, and R. J. Gildea, *Journal of Applied Crystallography*, 2009, **42**, 339-341.

15 A. L. Spek, *J. Appl. Cryst.*, 2003, **36**, 7; A. L. Spek, *Acta Crystallographica Section D Biological Crystallography*, 2009, **65**, 148.

16 N. A. Seaton, J. P. R. B. Walton and N. Quirke, *Carbon*, 1989, **27**, 853; J. Landers, G. Y. Gor and A. V. Neimark, *Colloids and Surfaces, A: Physicochemical and Engineering Aspects*, 2013, **437**, 3.

17 B. P. Russell and M. D. LeVan, *Carbon*, 1994, **32**, 845; R. W. Cranston and F. A. Inkley, in *Advances in Catalysis*, 1957, vol. 9, pp. 143.

18 G. P. Knowles, P. A. Webley, and Z. J. Liang, *Recent Advances in Post-Combustion CO_2 Capture Chemistry* (Ed. M Attalla), American Chemical Society, Symposium Series, 2012, **1097** (Ch 9), 177.

19 D. P. Arnold, *Polyhedron*, 1986, **5**, 1957; D. P. Arnold, *Journal of Chemical Education*, 1988, **65**, 1111.

20 S. J. Langford, M. A. P. Lee, and K. J. Macfarlane, *Journal of Inclusion Phenomena*, 2001, **41**, 135.

21 J.-S. Hu, Y.-G. Guo, and H.-P. Liang, *Journal of the American Chemical Society*, 2005, **127**, 17090; E. Deiters, V. Bulach and M. W. Hosseini, *Chemical Communications, (Cambridge, U. K.)*, 2005, 3906.

22 G. J. Kleywegt and T. A. Jones, *Acta Crystallographica, Section D: Biological Crystallography*, 1994, **D50**, 178.

23 J. C. Groen, L. A. A. Peffer and J. Perez-Ramirez, *Microporous and Mesoporous Materials*, 2003, **60**, 1.

24 W. Yang, A. Greenaway, and X. Lin, *Journal of the American Chemical Society*, 2010, **132**, 14457.

25 C. Larabi, P. K. Nielsen, and S. Helveg, *ACS Catalysis*, 2012, **2**, 695.

26 A. Kuc, T. Heine, and G. Seifert, *Chemistry - A European Journal*, 2008, **14**, 6597.

27 J. Lu, C. Perez-Krap, and M. Suyetin, *Journal of the American Chemical Society*, 2014, **136**, 12828.

28 A. Demessence, D. M. D'Alessandro, and M. L. Foo, *Journal of the American Chemical Society*, 2009, **131**, 8784; C. Knöfel, J. Descarpentries, A. Benzaouia, and V. Zeleňák, *Microporous and Mesoporous Materials*, 2007, **99**, 79, K. S. Walton, A. R. Millward, and D. Dubbeldam, *Journal of the American Chemical Society*, 2008, **130**, 406.

29 U. Englert, *Symmetry Relationships between Crystal Structures. Applications of Crystallographic Group Theory in Crystal Chemistry by Ulrich Mueller*, 2013, **52**, 11973.

30 H.-L. Jiang, D. Feng, and K. Wang, *Journal of the American Chemical Society*, 2013, **135**, 13934.

31 G.-Q. Guo, J.-F. Bai, H. Xing, Y.-Z. Li, and X.-Z, You, *Crystal Growth and Design*, 2006, **6**, 1264.

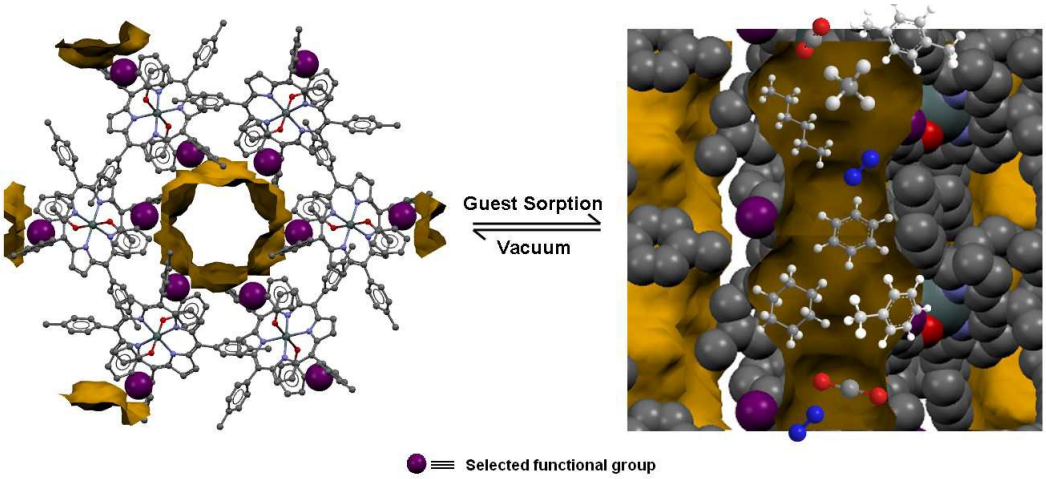

Supramolecular porphyrin network described in this paper revealed exceptional skeleton robustness as examined by N_2, CH_4, CO_2 gases sorption studies. Their pore size as well as surface properties of the channels can be successfully tuned by modification of the discrete porphyrin diphenolate molecules while the whole framework configuration was maintained during crystallization. Further investigation of the solvent vapor uptake revealed single crystal to single crystal transformation, which implies solvent purification based on supramolecular assembled porphyrin molecules can be warranted.